JPE 9-6-12

High Efficiency Soft-Switching Boost Converter Using a Single Switch

Jun-Ho Kim*, Doo-Yong Jung*, Sang-Hoon Park*, Chung-Yuen Won†, Yong-Chae Jung**, and Su-Won Lee*

*†School of Information and Communication Engineering, Sungkyunkwan University, Suwon, Korea
**Department of Electronic Engineering, Namseoul University, Cheonan, Korea

ABSTRACT

This paper presents a new soft-switching boost converter based on the *LC* resonance and passive clamping technique without additional active switches. The circuit achieves high efficiency and low voltage stress by adopting a soft switching method using *LC* resonance. This paper gives a mathematical analysis of each mode and a detailed design procedure of the proposed boost converter. First of all, the operational principles are verified through simulation results. Then, according to the design procedure, we designed and built a 1.5[kW] prototype soft switching boost converter. Through the experimental results, we demonstrated the validity and usefulness of the proposed boost converter.

Keywords: Soft-switching boost converter, Single switch, Resonance, ZVS, ZCS

1. Introduction

Nowadays, switch mode power conversion circuits and systems are being used effectively in renewable energy applications such as photovoltaic, fuel cell and wind-power generation systems, due to major advances in power semiconductor switching devices and their peripheral technologies [1~3]. To reduce the switching losses of DC-DC converters, the soft-switching technique (zero voltage switching or zero current switching) has been researched [4~8]. These converters have an auxiliary circuit, connected in parallel with the main switch, to help it turn-on under the zero voltage switching (ZVS) condition and a snubber capacitor to help the switch turn-off under the ZVS condition. The auxiliary circuit operates for only a small portion of the switching cycle and it is activated just before the main switch turn on. As a result, the system operates as a conventional PWM converter while reducing switching losses.

Although these converters have the advantage of improved efficiency, by applying the ZVS or zero current switching (ZCS) technique, they require additional switches and have the added complexity of a control circuit. Consequently, it could be difficult for these methods to be adopted by industry due to the cost of the additional switches and the complex control circuit.

A single switch resonant converter has been reported as a possible solution to this problem [9]. However, this topology exhibits high voltage stress while the switch is turned-off. This stress decreases efficiency and introduces EMI.

A soft switching boost converter is proposed, which is constructed based on the *LC* elements and the passive clamping diode, without additional active switches. Due to the soft switching technique for a single switch, this

Manuscript received April 10, 2009; revised Sept. 30, 2009
†Corresponding Author: won@yurim.skku.ac.kr
Tel: +82-31-290-7115, Fax: +82-31-299-4623, Sungkyunkwan Univ.
*School of Information & Communication Eng. Sungkyunkwan Univ.
**Department of Electronic Eng., Namseoul Univ.

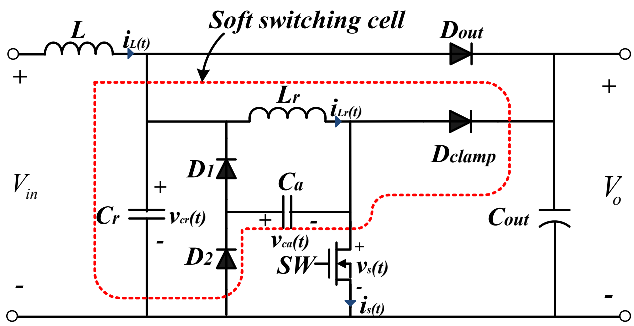

Fig. 1. Proposed soft switching boost converter.

proposed topology raises efficiency and minimizes switching losses, while the high voltage switching stress is reduced and the efficiency of the system is improved. In this paper the operational principles are explained through a mathematical analysis of the operation characteristics and a detailed design is also provided. The validity of the proposed design for a 1.5[kW], 30[kHz] soft-switching boost converter prototype is demonstrated through simulations and experiments.

2. Proposed Soft Switching Boost Converter

The circuit diagram of a boost converter employing a soft switching cell is shown in Fig. 1. The soft switching cell consists of one inductor, two capacitors and three diodes, and it is added to a conventional boost converter circuit. On/off control is achieved with one switch, and the switching loss can be reduced by switching at zero-current and zero-voltage, due to the resonances of L_r, C_a and C_r.

The following assumptions were made to simplify the steady state analysis of the circuit, shown in Fig. 1, during one switching cycle.

1. All switching devices and passive elements are ideal.
2. The parasitic components of all switching devices and elements are ignored.
3. All equations are derived, assuming that the starting point of each mode is zero.

Eleven stages occurred during steady state operation of the proposed converter through one switching cycle. Key waveforms concerning the operation stages are shown in Fig. 2. The operation can be analyzed as 11 modes according to the operating conditions defined in the following paragraphs.

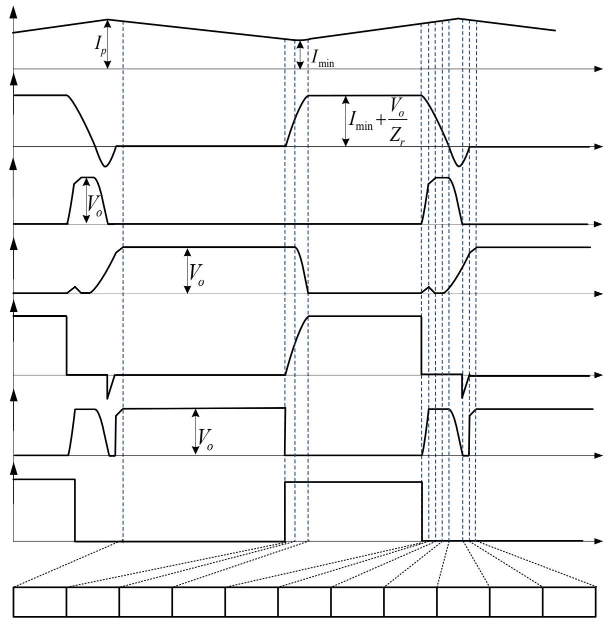

Fig. 2. Key waveforms of the proposed circuit.

Mode 1 ($t_0 \le t < t_1$): The switch is in the off state and dc input power is transmitted directly to the load through L and D_{out}. During this time, the main inductor voltage becomes $-(V_o - V_{in})$. Thus, the main inductor current decreases linearly.

$$i_L(t) = i_L(t_0) - \frac{V_o - V_{in}}{L} t \quad (1)$$

$$i_{Lr}(t) = 0 \quad , \quad v_{Cr}(t) = V_o \quad , \quad v_{Ca}(t) = 0 \quad (2)$$

$$i_L(t_1) = I_1 \quad (3)$$

Mode 2 ($t_1 \le t < t_2$): If the switch turns on under the ZCS condition, mode 2 starts. In this case, as the output voltage is supplied to the resonant inductor L_r and the current increases linearly. If this current reaches the same level as the current of the main inductor L, the current of the output side diode D_{out} becomes zero.

$$i_L(t) = I_1 - \frac{V_o - V_{in}}{L} t \quad (4)$$

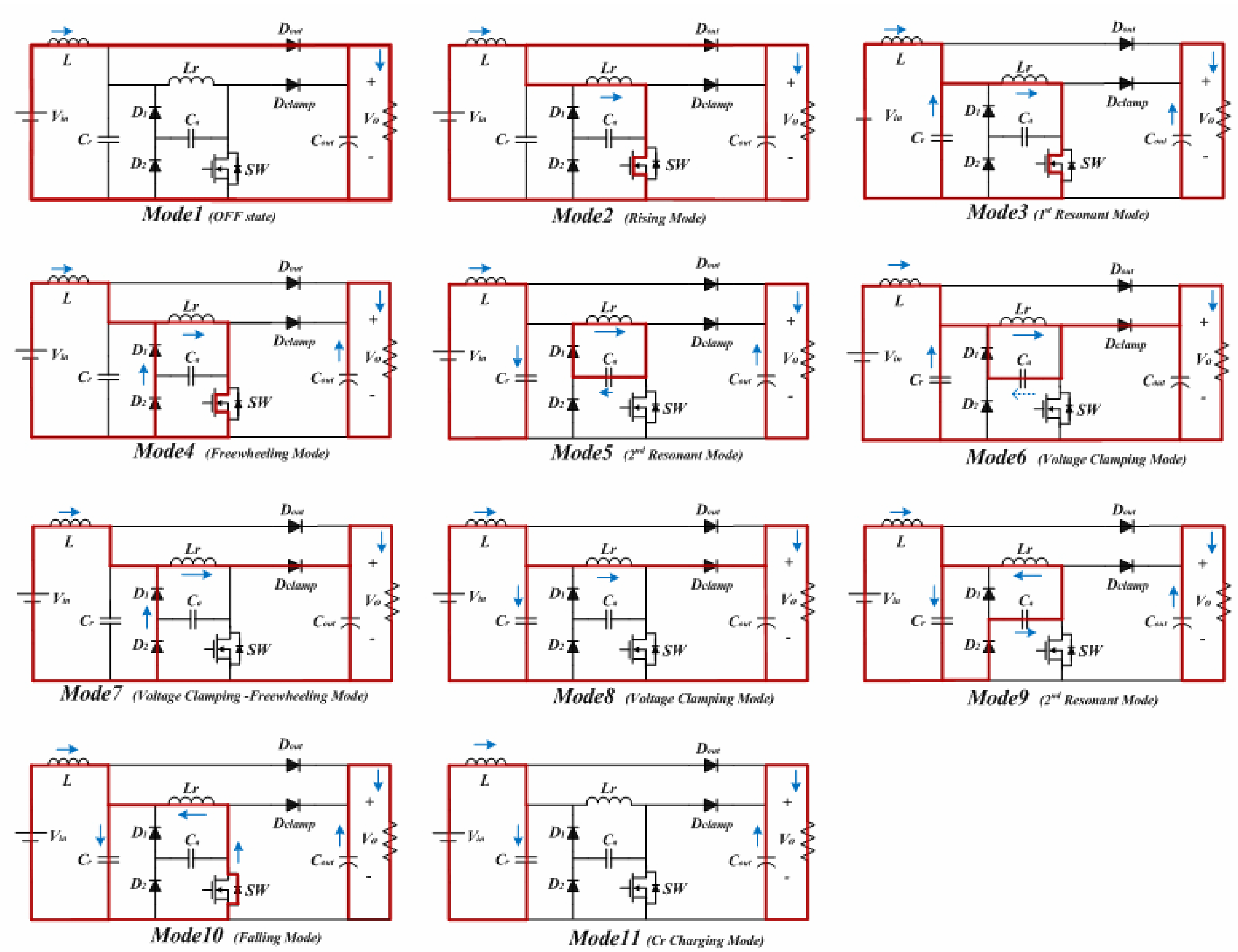

Fig. 3. Operational modes of the proposed converter.

$$i_{Lr}(t) = \frac{V_o}{L_r} t \quad , \quad v_{Cr}(t) = V_o \quad , \quad v_{Ca}(t) = 0 \qquad (5)$$

$$i_L(t_2) \approx I_{\min} \quad , \quad i_{Lr}(t_2) \approx I_{\min} \qquad (6)$$

Mode 3 ($t_2 \le t < t_3$,** 1st Resonant Mode**): If the current of D_{out} becomes zero and turns off, the resonant mode starts. In this mode, the resonant inductor L_r and the capacitor C_r resonate and the voltage of C_r falls from the output voltage V_o to zero. In this case, the current of the main inductor L flows through L_r and the switch. The load is supplied with power continuously as the voltage at C_{out} discharges.

$$i_L(t) \approx I_{\min} \quad , \quad v_{Ca}(t) = 0 \qquad (7)$$

$$i_{Lr}(t) = I_{\min} + \frac{V_o}{Z_r} \sin \omega_r t \qquad (8)$$

$$v_{Cr}(t) = V_o \cos \omega_r t \qquad (9)$$

$$i_{Lr}(t_3) = I_2 \quad , \quad v_{Cr}(t_3) = 0 \qquad (10)$$

where the characteristic impedance Z_r and the resonant angular frequency ω_r are defined in Eq. (11).

$$\omega_r = 1/\sqrt{L_r C_r} \quad , \quad Z_r = \sqrt{L_r / C_r} \qquad (11)$$

Mode 4 ($t_3 \le t < t_4$,** 1st Freewheeling Mode**): If the resonant capacitor voltage becomes zero, the two auxiliary diodes D_1 and D_2 turn on, and the freewheeling mode starts. While in this mode, the resonant inductor current is composed of two currents: the main inductor current and the current through the two auxiliary diodes. The main inductor current increases linearly.

$$i_L(t) = I_{\min} + \frac{V_{in}}{L}t \tag{12}$$

$$i_{Lr}(t) \approx I_2 \tag{13}$$

$$v_{Cr}(t) = 0 \quad , \quad v_{Ca}(t) = 0 \tag{14}$$

$$i_L(t_4) = I_3 \quad , \quad i_{Lr}(t_4) = I_2 \tag{15}$$

Mode 5 ($t_4 \le t < t_5$, 2nd Resonant Mode): At t_4, as a result of the PWM algorithm, the switch turns off at the zero voltage condition. At this time, there are two current loops. One is the L-C_r-V_{in} loop where the voltage of capacitor C_a increases linearly from zero to the output voltage V_o. The other is the L_r-C_a-D_1 loop where the second resonance takes place. The energy stored in L_r moves to C_a.

$$i_L(t) = I_3 + \frac{V_{in}}{L}t \tag{16}$$

$$i_{Lr}(t) = I_2 \cos\omega_a t \tag{17}$$

$$v_{Ca}(t) = Z_a I_2 \sin\omega_a t \tag{18}$$

$$v_{Cr}(t) = \frac{I_3}{C_r}t \tag{19}$$

$$i_L(t_5) = I_4 \quad , \quad i_{Lr}(t_5) = I_5 \quad , \quad v_{Cr}(t_5) = V_1 \tag{20}$$

where the characteristic impedance Z_a and the resonant frequency ω_a are defined in Eq. (21).

$$\omega_a = 1/\sqrt{L_r C_a} \quad , \quad Z_a = \sqrt{L_r / C_a} \tag{21}$$

Mode 6 ($t_5 \le t < t_6$): If the voltage of SW is equal to V_o, D_{clamp} is turned on, the peak voltage across switch *SW* is clamped to V_o, and the L_r current flows into C_a and D_{clamp}. Since the current of C_a is very small, most of the L_r current flow into D_{clamp}. In this mode, the energy of inductor L_r is transferred to capacitor C_{out}.

$$i_L(t) = I_4 + \frac{V_{in}}{L}t \tag{22}$$

$$v_{Ca}(t) = (V_o - V_1)\cos\omega_p t + Z_p(t_5 - t_4)\sin\omega_p t \tag{23}$$

$$v_{Cr}(t) = V_o - (V_o - V_1)\cos\omega_p t - Z_p(t_5 - t_4)\sin\omega_p t \tag{24}$$

$$i_{Lr}(t) = I_4 + (I_5 - I_4)\cos\omega_p t - \frac{V_o - V_1}{Z_p}\sin\omega_p t \tag{25}$$

$$i_L(t_6) = I_6 \quad , \quad i_{Lr}(t_6) = I_7 \tag{26}$$

where $\omega_p = 1/\sqrt{L_r C_p}$, $Z_p = \sqrt{L_r / C_p}$, $C_r + C_a = C_p$.

Mode7 ($t_6 \le t < t_7$): The voltage of C_r is zero. The main inductor current i_L flows to C_{out} through L_r. Another current path is D_1-D_2-L_r-D_{clamp}-C_{out} and the current i_{Lr} is ($i_L + i_{D1}$). This stage is described by Eqs. (27) ~ (30).

$$i_L(t) = I_6 + \frac{V_o - V_{in}}{L}t \tag{27}$$

$$i_{Lr}(t) = I_7 - \frac{V_o}{L_r}t \tag{28}$$

$$v_{Ca}(t) = V_o \quad , \quad v_{Cr}(t) = 0 \tag{29}$$

$$i_L(t_7) = I_8 \quad , \quad i_{Lr}(t_7) = I_9 \tag{30}$$

Mode 8 ($t_7 \le t < t_8$): If two inductor currents become equal, the main inductor current is divided between C_r and L_r. Until the current I_{Dclamp} becomes zero, the energy of L_r is transmitted to C_{out}. The state equations are as follows:

$$i_L(t) = I_8 + \frac{V_o - V_{in}}{L}t \tag{31}$$

$$v_{Cr}(t) = V_o - V_o \cos\omega_r t \tag{32}$$

$$v_{Ca}(t) = V_o \tag{33}$$

$$i_{Lr}(t) = I_9 - \frac{V_o}{Z_r}\sin\omega_r t \tag{34}$$

$$i_L(t_8) = I_p \quad , \quad i_{Lr}(t_8) = 0 \quad , \quad v_{Cr}(t_8) = V_2 \tag{35}$$

Mode9 ($t_8 \le t < t_9$): In mode 9, the voltage of C_a decreases. It also continuously resonates the D_2-C_a-L_r-C_r

loop and the energy moves from C_a to L_r. If the voltage of C_a becomes zero, the current of L_r reverses from the current direction of mode 5. If the voltage of C_a becomes zero, the anti-parallel diode of the switch turns on and it turns over to the next mode. The state equations are:

$$i_L(t) = I_p \tag{36}$$

$$i_{Lr}(t) = \frac{C_s}{C_r} I_p (1-\cos\omega_s t) - \frac{V_o - V_2}{Z_r}\sin\omega_s t \tag{37}$$

$$\begin{aligned} v_{Cr}(t) &= V_2 + \frac{C_s}{C_r}(V_o - V_2)(1-\cos\omega_s t) \\ &+ \frac{I_p}{C_p}t + \frac{C_s I_p}{C_r{}^2\omega_s}\sin\omega_s t \end{aligned} \tag{38}$$

$$\begin{aligned} v_{Ca}(t) &= V_o - \frac{C_s}{C_a}(V_o - V_2)(1-\cos\omega_s t) \\ &+ \frac{I_p}{C_p}t - \frac{I_p}{C_p\omega_s}\sin\omega_s t \end{aligned} \tag{39}$$

$$v_{Cr}(t_9) = V_3 \ , \ i_{Lr}(t_9) = I_{10} \tag{40}$$

where $C_s = C_r C_a/(C_r + C_a)$, $Z_s = \sqrt{L_r/C_s}$, $\omega_s = 1/\sqrt{L_r C_s}$.

Mode 10 ($t_9 \le t < t_{10}$): In mode 10, there are also two current loops. The current of the main inductor L charges C_r and decreases linearly. The current of the resonant inductor L_r transmits its energy to the capacitor C_r and flows through the anti-parallel diode of the switch. If the current of the inductor L_r becomes zero, mode 10 ends.

$$i_L(t) = I_p + \frac{V_3 - V_{in}}{L}t \tag{41}$$

$$i_{Lr}(t) = I_p - (I_p + I_{10})\cos\omega_r t + \frac{V_3}{Z_r}\sin\omega_r t \tag{42}$$

$$v_{Cr}(t) = V_3\cos\omega_r t + Z_r(I_p - I_{10})\sin\omega_r t \tag{43}$$

$$v_{Ca}(t) = 0 \tag{44}$$

$$i_L(t_{10}) = I_{11}, \ i_{Lr}(t_{10}) = 0, \ v_{Cr}(t_{10}) = V_4 \tag{45}$$

Mode 11 ($t_{10} \le t < t_{11}$): If the voltage of C_r is less than the output voltage V_o, mode 11 occurs. Input or main inductor current charges the capacitor C_r. In this mode, the voltage of C_r is the same as the voltage of the switch.

$$i_L(t) = I_p - \frac{V_4 - V_{in}}{L}t \tag{46}$$

$$i_{Lr}(t) = 0 \ , \ v_{Ca}(t) = 0 \tag{47}$$

$$v_{Cr}(t) = V_4 + \frac{I_{11}}{C_r}t \tag{48}$$

3. ZVS Condition and Design Procedures

3.1 ZVS Condition

Fig. 4 shows the key waveforms of the soft-switching boost converter.

To satisfy the ZVS condition, the resonant inductor current must be larger than the main inductor current during the freewheeling interval of mode 4. The ZVS condition of the proposed converter is expressed by:

$$I_2 > I_p \tag{49}$$

where $I_2 = I_{min} + V_o/Z_r$, $I_p = I_{min} + \Delta I_L$,

$$\frac{V_o}{Z_r} > \Delta I_L \tag{50}$$

where $\Delta I_L = I_L / 2.5$.

In mode 5(t_4-t_5), the ZVS area depending on L_r and C_a can be extended or reduced. As a result, Eq. (18) can be expressed by Eq. (51).

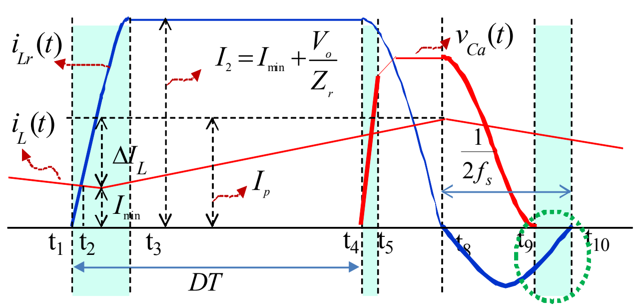

Fig. 4. Key waveforms of ZVS condition.

$$v_{Ca}(t) = \sqrt{\frac{L_r}{C_a}} I_2 \sin \frac{1}{\sqrt{L_r C_a}} t \tag{51}$$

To satisfy the ZVS condition in mode 10, the voltage of C_a must be less than zero at t_{10}, as shown in Eq. (52).

$$v_{Ca}(t_{10}) < 0 \tag{52}$$

Therefore, Eq. (39) can be expressed by Eq. (53).

$$V_o - 2\frac{C_r // C_a}{C_a}(V_o - V_2) + \frac{I_p}{C_r + C_a}\pi\sqrt{L_r C_r // C_a} < 0 \tag{53}$$

where $t = 1/2f_s = \pi\sqrt{L_r C_r // C_a}$.

3.2 Selection of Resonant Elements (C_a, C_r & L_r)

When the switch turns off, it provides an alternative path for the main inductor current to reduce switching losses. Since the snubber capacitor incorporates the output capacitance of the switch, the exact capacitance value selected will be affected by the semiconductor devices employed. Usually, a snubber capacitor is selected that has a capacitance value that is more than ten times larger than the output capacitance C_{oss} of the switch. However, in this topology the capacitor C_a is charged by the resonant inductor current i_{Lr}. As a result, it can be more than twice the main inductor current i_L during switch turn off. Thus, the snubber capacitance value can be 20 times larger than the output capacitance of the switch, and the expression can be written as follows:

$$C_a > 20C_{oss} \tag{54}$$

The resonant inductor current in mode 3, is expressed in Eq. (8). The time duration of mode 3, which is the resonant time of the resonant inductor L_r and the resonant capacitor C_r, is defined as one-fourth of the resonant period. Usually, the rising time of the resonant inductor current i_{Lr} can be set to 10% of the minimum on time but we set it to 50%, because in this topology the capacitance of C_r should be greater than C_a to obtain the ZVS condition. Therefore the following equation can be expressed:

$$t_3 - t_1 = \frac{L_r}{V_o} I_{\min} + \frac{T_r}{4} < 0.5 D_{\min} T \tag{55}$$

where $T_r = 1/f_s = 2\pi\sqrt{L_r C_r}$, $T = 1/f_{SW}$, $D_{\min} = (V_o - V_{in\_min})/V_o$

Solving Eq. (55), the value of the resonant capacitor C_r can be found.

$$C_r > \frac{D_{\min}{}^2}{\pi^2 L_r f_{SW}{}^2} + \frac{I_{\min}{}^2 L_r}{\pi^2 V_o{}^2} - \frac{2 I_{\min} D_{\min}}{\pi^2 V_o f_{SW}{}^2} \tag{56}$$

Since $(2 I_{\min} D_{\min}) / (\pi^2 V_o f_{SW}{}^2) \approx 0$ in Eq. (56), this equation can be written as:

$$C_r > \frac{D_{\min}{}^2}{\pi^2 L_r f_{SW}{}^2} + \frac{I_{\min}{}^2 L_r}{\pi^2 V_o{}^2} \tag{57}$$

$$L_r = \{V_o / (I_2 - I_{\min})\}^2 C_r \tag{58}$$

where $I_2 - I_{\min} = V_o / Z_r = V_o \sqrt{C_r} / \sqrt{L_r}$

From Eq. (57) and (58), C_r can be defined as:

$$C_r > \frac{D_{\min}(I_2 - I_{\min})}{\pi^2 V_o f_{SW}{}^2} / \sqrt{1 - I_{\min}{}^2 / \pi^2 (I_2 - I_{\min})^2} \tag{59}$$

From Eq. (58), the resonant inductor value is expressed as:

$$L_r < \left\{(2 \times 0.85 \frac{C_s}{C_a} - 1) V_o / (\frac{I_p}{C_r + C_a} \pi \sqrt{C_s})\right\}^2 \tag{60}$$

where $C_s = C_r C_a / (C_r + C_a)$, $V_o - V_2 \approx 0.85 V_o$.

3.3 Design Procedures and Examples

Based on the derived equations, the design procedure for the proposed converter is summarized in this section. Table 1 shows the principal design parameters of the proposed boost converter. The design guidelines are presented to aid in the choice of resonant components to ensure appropriate operation of the resonance converter.

Table 1. Design parameters.

Parameter	Symbol	Value	Unit
Input voltage	V_{in}	200~350	Vdc
Output voltage	V_o	400	Vdc
Input power	P_{in}	1.6	kW
Output power	P_o	1.5	kW
Efficiency	η	95	%
Switch output capacitance	C_{oss}	320	pF
Switching frequency	f_{sw}	30	kHz

According to Table 1, the main inductor average and ripple current values are as follows:

$$I_L = \frac{P_{in}}{V_{in\_min}} = \frac{1{,}600}{200} = 8\,\text{A} \quad (61)$$

$$\Delta I_L = \frac{I_L}{2.5} = \frac{8}{2.5} = 3.2\,\text{A} \quad (62)$$

The maximum and minimum main inductor currents (I_p and I_{min}) are:

$$I_P = I_L + \frac{\Delta I_L}{2} = 8 + \frac{3.2}{2} = 9.6\,\text{A} \quad (63)$$

$$I_{\min} = I_L - \frac{\Delta I_L}{2} = 8 - \frac{3.2}{2} = 6.4\,\text{A} \quad (64)$$

The duty ratio D and turn on time T_{on} of the switch are:

$$D_{\max} = \frac{V_o - V_{in\_\min}}{V_o} = \frac{400-200}{400} = 0.5 \quad (65)$$

$$D_{\min} = \frac{V_o - V_{in\_\max}}{V_o} = \frac{400-350}{400} = 0.125 \quad (66)$$

$$T_{on} = D_{\max} T = \frac{D_{\max}}{f_{SW}} = \frac{0.5}{30\times 10^3} = 16.667\times 10^{-6}\,\text{s} \quad (67)$$

Therefore, we can find the main inductance L as follows:

$$L = \frac{V_{in\_\min} T_{on}}{\Delta I_L} = \frac{200\times 16.667\times 10^{-6}}{3.2} = 1.042\,m\text{H} \quad (68)$$

From Eq. (54), we can calculate the range of the auxiliary resonant capacitor C_a as:

$$C_a > 20\cdot C_{oss} = 20\times 320\times 10^{-12} = 6.4\text{nF} \approx 10\text{nF} \quad (69)$$

To find C_r, we must select a value of I_2 which is less than the rating current of the switch. In this case, $I_2 = 23[A]$. From Eq. (59), we can also find the range of the resonant capacitor C_r as follows:

$$C_r > \frac{D_{\min}(I_2 - I_{\min})}{\pi\cdot V_o\cdot f_{SW}} / \sqrt{1 - I_{\min}{}^2/\pi^2(I_2 - I_{\min})^2} = \frac{0.125(23-6.4)}{400\pi\times 30\times 10^3\times 0.9778} = 56\text{nF} \approx 100\text{nF} \quad (70)$$

From Eq. (60) and (70), the range of values that can be used for the resonant inductor L_r is:

$$L_r < \left\{ (2\times 0.85\frac{C_s}{C_a} - 1)V_o / (\frac{I_p}{C_r + C_a}\pi\sqrt{C_s}) \right\}^2 = \left\{ (1.7\times\frac{9}{10} - 1)400/(\frac{9.6}{110\times\sqrt{10^{-9}}}\times 3\pi) \right\}^2 = 69\,\mu\text{H} \approx 50.6\,\mu\text{H} \quad (71)$$

where $C_s = C_r C_a / (C_r + C_a) = 100 \times 10 / (100 + 10) \approx 9\text{nF}$.

4. Simulation Results

We simulated the proposed soft-switching boost converter using PSIM Ver. 6.0 software. To verify the operation of the proposed topology, a simulation model based on a 1.5kW boost converter was used. The simulation parameters are shown in Table 2.

Table 2. Simulation parameters.

Parameter	Symbol	Value	Unit
Input voltage	V_{in}	200~350	Vdc
Output voltage	V_o	400	Vdc
Output power	P_o	1.5	kW
Main inductor	L	1,000	μH
Resonant inductor	L_r	50.6	μH
Resonant capacitor	C_r	100	nF
Auxiliary capacitor	C_a	10	nF
Input capacitor	C_{in}	900	μF
Output capacitor	C_{out}	750	μF
Switching frequency	f_{sw}	30	kHz

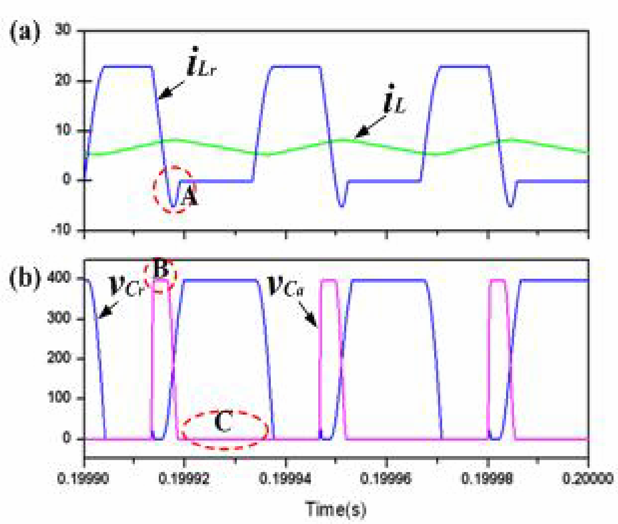

Fig. 5. Waveforms of i_L, i_{Lr}, v_{ca} and v_{cr} in the proposed topology.

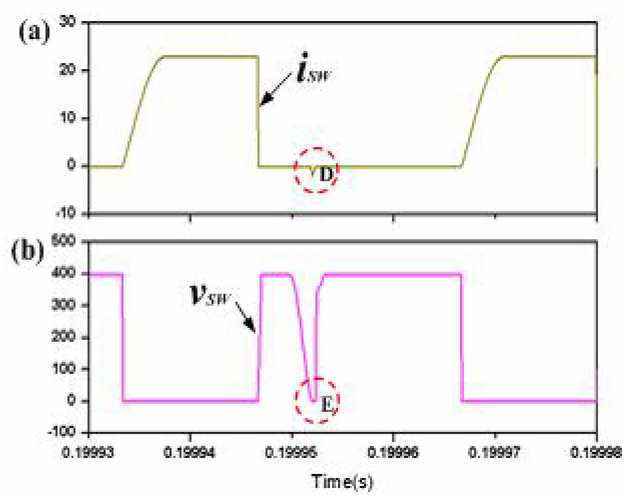

Fig. 6. The current and voltage waveforms of the switching device.

In Fig. 5(a), the current through the main inductor L increased and decreased linearly according to the on-off state of the switch. The resonant inductor also accumulated and released energy according to the state of the switch.

While the main switch is turned on, the main inductor accumulates energy. When the switch is turned off, this energy is transferred to the output. The current through L_r is more than twice the main inductor current, and it should drop below zero in area A. Fig. 5(b) shows the voltage waveforms of C_a and C_r. Due to the clamping diode D_{clamp}, area B shows the clamped voltage, where the voltage across the auxiliary capacitor C_a is clamped at V_o. In Fig. 5(b) the voltage of C_a drops down to zero in area C. Therefore ZVS on for the switch *SW* can be achieved.

Fig. 6 shows the waveforms of the switch current and voltage. Due to the anti-parallel diode of the switch, the current of the switch is reversed in area D. The voltage waveform of the switch should be similar to the shape of E. To satisfy the ZVS condition in Fig. 6(b), the voltage should drop to zero in area E.

5. Experimental Results

A prototype of a 1.5kW 30Hz boost converter was built to verify the operation principle and the theoretical analysis. This converter was regulated at 200Vdc ~ 350Vdc input and 400Vdc output. A CoolMOS

(IPW60R045CP) was used as the switching device. The key components used in the prototype and the operating conditions used for the test are shown in Table 2 and Table 3.

Table 3. Parameters of switch and diode.

Switch Part Number	I_D (25°C)	I_D (100°C)	V_{DS}	$R_{ds(on)}$ (max)
IPW60R045CP (CoolMOS)	25A	60A	600V	0.045Ω
Diode Part Number	I_F (95°C)	V_F (MAX)	V_{RRM} (MAX)	t_{rr} (1A,100A/μs)
80EPF06 (fast soft recovery)	80A	1.25V	600V	70ns

The key experimental waveforms of the proposed boost converter are shown in Fig. 7~10.

Fig. 7 shows the main and resonant inductor currents at full load. The waveforms obtained from the prototype are very close to those shown in Fig. 5(a).

Compared with the simulation result in Fig. 5(b), there is a charging voltage of C_a shown in area F of Fig. 8. The difference was caused by the output capacitance of the switch (IPW60R045CP).

Fig. 9 shows the waveforms of the main switch current and voltage. ZCS/ZVS operation and voltage clamping are demonstrated. The ZCS waveforms of the switch at turn on are shown in Fig. 10. It is clear that turn-on switching takes place under the ZCS condition, if we compare this with Fig. 11 which shows the waveforms of voltage and current in a conventional hard switching boost converter under the same operating conditions.

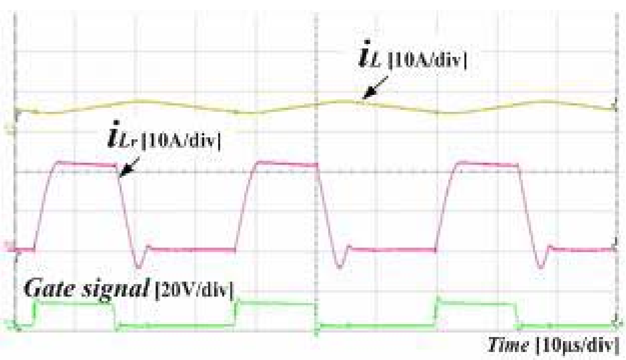

Fig. 7. Experimental result of current waveforms of L, L_r and gate signal.

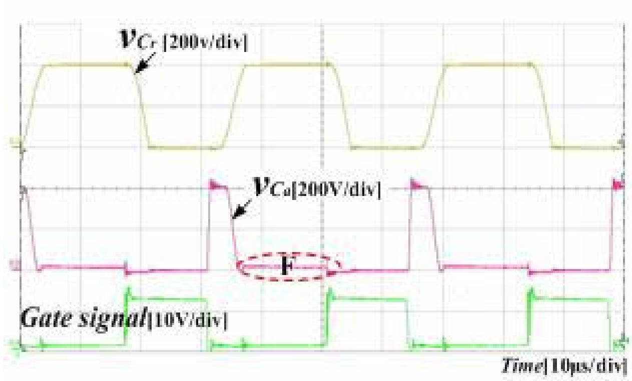

Fig. 8. Experimental result of voltage waveforms of C_r , C_a and gate signal.

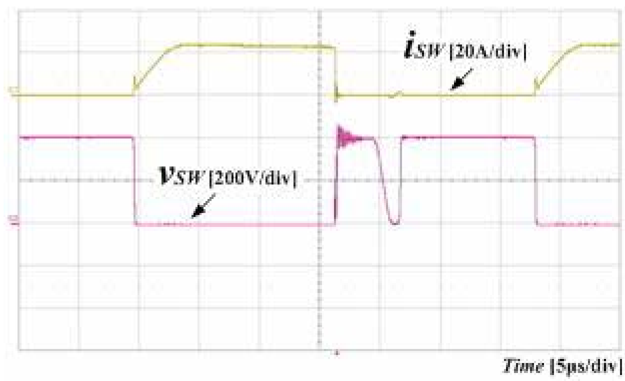

Fig. 9. Experimental waveforms of the current and voltage of switching device.

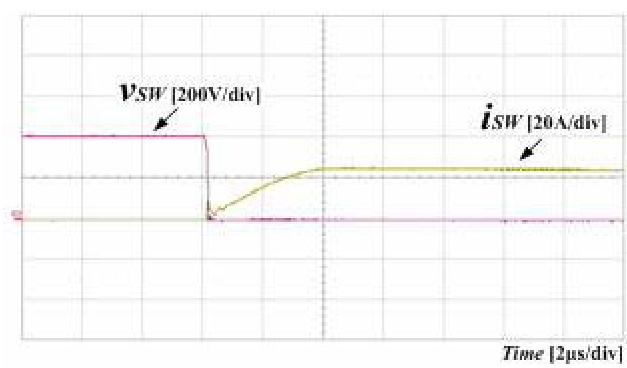

Fig. 10. Zero current switching waveforms.

Fig. 12 shows the efficiency of the proposed converter with duty and load variation. The measured maximum efficiency reached 97% under the full load condition.

Fig. 13 shows the efficiency of the conventional hard switching boost converter topology with duty and load variation. The measured maximum efficiency reached 95% under the full load condition.

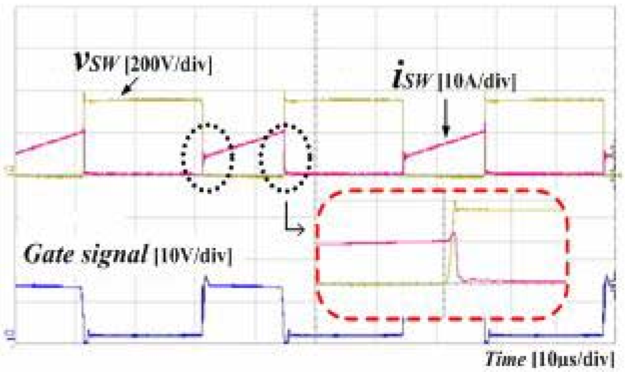

Fig. 11. Experimental result of voltage and current waveforms for conventional hard switching boost converter.

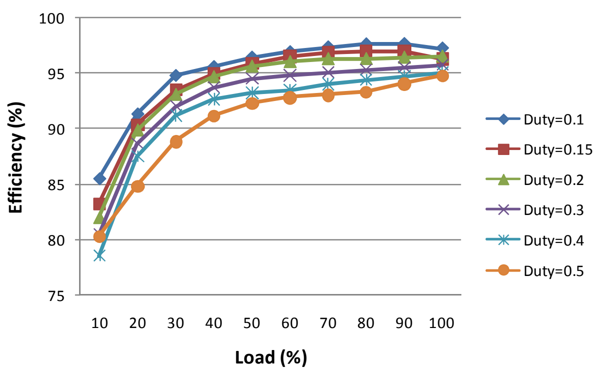

Fig. 12. The efficiency of the proposed boost converter topology.

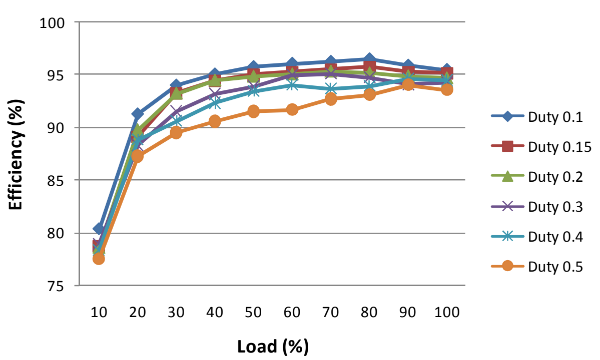

Fig. 13. The efficiency of the conventional (hard switching) boost converter topology.

6. Conclusions

This paper presents a soft-switching boost converter using resonance. It was constructed based on the proposed soft-switching cell designed using the *LC* resonance and passive clamping technique, without additional active switches. The proposed topology increases efficiency and reduces switching loss and high voltage stress. By analyzing the operation of this converter, the principles of this topology were proven. Using the soft-switching technique, the efficiency of the system is higher than 95% under the full load condition. The circuit composition and operational principles were explained through a mathematical analysis of each mode, and a detailed description of the proposed boost converter was provided. This paper analyzed the operational characteristics of the topology and presented detailed design procedures. The validity of the proposed design was demonstrated by building a 1.5[kW], 30[kHz] soft-switching boost converter prototype regulated at 200[V] dc input and 400[V] dc output and experimentally verifying the analysis.

Acknowledgment

This work was the outcome of a Manpower Development Program for Energy & Resources supported by the Ministry of Knowledge and Economy (MKE).

References

[1] Soon Kurl Kwon, Khairy F.A.Sayed "Boost-half bridge single power stage PWM DC-DC converters for PEM-fuel cell stacks," *Journal of Power Electronics*, Vol. 8, No. 3, pp. 239-247, July, 2008.

[2] Jong-Pil Lee, Byung-Duk Min, Tae-Jin Kim, Dong-Wook yoo, Ji-Yoon Yoo, "Design and Control of Novel Topology for photovoltaic dc/dc converter with high efficiency under wide load ranges," *Jounal of Power Electronics,* Vol. 9, No. 2, pp. 300-307, March, 2009.

[3] Byung-Duk Min, Jong-Pil Lee, Jong-Hyun Kim, "A novel grid-connected PV PCS with new high efficiency converter," *Jounal of Power Electronics,* Vol. 8, No. 4, pp. 309-316, Oct. 2008.

[4] Ghodke D.V. and Muralikrishnan, K., "1.5 kW two switch forward ZCZVS converter using primary side clamping," *IEEE PESC'02*, pp. 893-898, June 2002.

[5] Barb I. Vieira, J.B., Jr. Hey, H.L. "A pulse-width modulation zero-voltage-zero-current switched half-bridge quasi-resonant converter," *IEEE IECON'89*, pp. 42-47, Nov. 1989.

[6] Tae-Woo Kim, Hack-Sung Kim, Hee-Wook Ahn, "An improved ZVT PWM boost converter," *IEEE PESC'00*, pp. 615-619, Nov. 2000.

[7] Ivanovic B., Stojiljkovic Z., "A novel active soft switching snubber designed for boost converter," *IEEE Transactions on Power Electronics*, Vol. 1, Issue 3 pp. 658-665, May 2004.

[8] Chung H., Hui S.Y.R., Tse K.K., "Reduction of power converter EMI emission using soft-switching technique," *IEEE Transactions on Electromagnetic Compatibility*, Vol. 40, Issue 3, pp. 282-287, Aug. 1998.

[9] Jun-Ho Kim, Doo-Yong Jung, Jae-Hyung Kim, Su-Won Lee, Yong-Chae Jung and Chung-Yun Won, "Soft switching interleaved boost converter for photovoltaic power generation system," *IEEE ICSET'08*, pp. 257-262, Nov. 2008.

Jun-Ho Kim was born in Korea in 1971. He received B.S. and M.S. degrees in Electrical Engineering from Sungkyunkwan University, Suwon, Korea, in 1998 and 2001, respectively. He has been working towards his Ph.D. Since 2001, he has been working for the Korean Agency for Technology and Standards (KATS), MKE. His research interests include testing methods and the safety of the converter systems in the areas of renewable energy and rotating machinery.

Doo-Yong Jung was born in Korea in 1981. He received a B.S degree in Electrical Electronics Engineering from Anyang University, Anyang, Korea, in 2007, and a M.S. degree in Photovoltaic System Engineering from Sungkyunkwan University, Suwon, Korea, in 2009. Since 2009, he has been working towards his Ph.D. His main research interests include converters, inverters, and battery chargers.

Sang-Hoon Park was born in Korea in 1979. He received a M.S degree in Information and Communication Engineering from Sungkyunkwan University, Suwon, Korea, in 2007. He is currently working toward his Ph.D. in Electronics and Electrical Engineering at Sungkyunkwan University. His research interests include converters, inverters, electrical vehicle systems and generator systems.

Chung-Yuen Won was born in Korea in 1955. He received a B.S. degree in Electrical Engineering from Sungkyunkwan University, Suwon, Korea, in 1978, and a M.S. and a Ph.D. in Electrical Engineering from Seoul National University, Seoul, Korea, in 1980 and 1988, respectively. From 1990 to 1991, he was with the Department of Electrical Engineering at the University of Tennessee, Knoxville, as a Visiting Professor. Since 1988, he has been with the faculty of Sungkyunkwan University, where he is currently a Professor in the School of Information and Communication Engineering. He is also the president of the Samsung Energy Power Research Center. His research interests include dc-dc converters for fuel cells, electro-magnetics modeling and prediction for motor drives, and control systems for rail power delivery applications. Dr. Won is a member of the Institute of Electrical and Electronics Engineers (IEEE).

Yong-Chae Jung was born in Korea in 1965. He received a B.S. degree from Hanyang University, Seoul, Korea, in 1989, and a M.S. and a Ph.D. in Electrical Engineering from the Korea Advanced Institute of Science and Technology (KAIST), Daejeon, Korea, in 1991 and 1995, respectively. He is currently an associate professor in the Department of Electronic Engineering at Namseoul University. His research interests include the design and control of power converters, soft switching power converters, resonant power circuits, photovoltaic systems, power factor corrections, SMPS, induction heating circuits and EMI suppression. Dr. Jung is a member of the Korea Institute of Power Electronics (KIPE), and the Korea Institute of Electrical Engineering (KIEE).

Su-Won Lee received his B.S., M.S. and Ph.D. in Electrical Engineering from Chonbuk National University, Korea in 1991, 1993 and 1998 respectively. He was a Research Professor with the BK21 Research Team at Kunsan National University from 2001 to 2006. He was a Research Professor with the Institute of TMS Information Technology at Yonsei University from 2006 to 2008. Currently, he is a research professor with the Center for Advanced IT HRD with Close Industry Cooperation at Sungkyunkwan University. His research interests include bi-directional dc/dc converters, inverter controls and renewable energy based distributed generation systems.